Journal of Inorganic and General Chemistry
ZAAC
Zeitschrift für anorganische und allgemeine Chemie
DOI: 10.1002/zaac.202000306
ARTICLE

Re-investigation of Barium-Gold(I)-Tetra-Thiostannate(IV), $Ba[Au_2SnS_4]$, with Short $Au^I\cdots Au^I$ Separation Showing Luminescence Properties

Christoph Ludwig Teske,*[a] Huayna Terraschke,[a] Sebastian Mangelsen,[a] and Wolfgang Bensch[a]

Abstract. New investigations combining single crystal- and synchrotron-based powder X-ray diffraction data revealed that $Ba[Au_2SnS_4]$ crystallizes in the orthorhombic crystal system in space group $C222_1$ instead of $P2_12_12$ as reported earlier. While the principle crystal structure is not altered, there are significant differences of the interatomic distances Au-S and Sn-S. A salient property of this crystal structure is the partial framework composed of AuS_2 dumbbells and SnS_4 tetrahedra to form chains $[(Au_2SnS_4)^{2-}]_\infty$ propagating in the [100] direction. Within the chains a short Au···Au separation of 2.9538(13) Å is observed, while the interchain Au···Au separation is longer at 3.383 Å. The Ba^{2+} cation is eightfold coordinated by S^{2-} anions in a distorted bicapped trigonal prismatic environment BaS_8. These polyhedra share all S^{2-} anions thus generating a three-dimensional network. This connection Scheme generates voids along [100] hosting $[(Au_2SnS_4)^{2-}]_\infty$ chains. In addition, the compound has been shown to be luminescent at the blue-green spectral range with emission maximum at approximately 21000 cm^{-1}.

Introduction

Thiostannate anions feature a variety of building units like e.g. $[SnS_4]^{4-}$, $[Sn_2S_6]^{4-}$, $[Sn_2S_5]^{2-}$, $[Sn_2S_7]^{6-}$, $[Sn_2S_8]^{2-}$, $[Sn_3S_7]^{2-}$, $[Sn_4S_9]^{2-}$, $[Sn_4S_{10}]^{4-}$, or $[Sn_5S_{12}]^{4-}$. Charge compensation is achieved by different cations including main group metal cations,[1–9] combinations of main group and transition metal cations,[10–22] transition metal cations and/or complexes,[23–34] and organic ammonium and/or metal cations.[35–40] Several of these compounds exhibit interesting physico-chemical properties like second harmonic generation,[17,18] efficient ion exchange behavior for rare earth cations,[41] promising properties as anode materials in lithium ion batteries,[39] selective heavy metal cation sequestration from aqueous solutions,[8] photoconductivity,[28] or photocatalytic activity for dye degradation,[30] to name just a few. Comparing the pure inorganic thiostannates the chalcophilic elements e.g. Cu, Ag, or Au seem to be easily integrated in such compounds forming tetrahedral scaffolding structures. Thiostannate compounds with Au are rare, and until now, only $Cs_2Au_2SnS_4$,[42] $K_2Au_2SnS_4$ and $K_2Au_2Sn_2S_6$[43] and $BaAu_2SnS_4$[21] were reported.

In all these compounds, the Au···Au separations are relatively short at about 3 Å indicating weak interactions. These interatomic Au–Au distances are comparable with the distance in elemental gold (2.8782 Å[44]). The nature of the interaction responsible for occurrence of short Au–Au distances was strongly debated since the late 1980's.[45,46] Finally, the terms *aurophilic bonding* or *aurophilicity* were created.[47–51] The title compound, having also comparable short Au–Au distances, was one of most early examples mentioned during this discussion.[45] Furthermore, Au^I compounds are interesting luminescence materials, since the aurophilic interaction is involved as a source of the emission process.[52–55] Luminescence, on the one hand, depends on structural features like e.g. pairs, rings, chains, or layers[56] and the type of ligands. Otherwise, it was suggested that the emission energy should also correlate with the inverse of the Au–Au distance.[57,58] Actually, these correlations are complex. However, in *very simplified* terms it seems likely that with increasing Au–Au distances implying decreasing aurophilic interactions, the emission energy declines and vice versa. Structure–luminescence relationship is a central issue for the development of luminescent materials.

Recently, we synthesized and characterized the compound mono(dithiocarbamato)-gold(I), AuS_2CNH_2.[59] The crystal structure of this compound features infinite Au chains linearly coordinated by two sulfur atoms of the dithiocarbamate moiety [Au–Au = 3.2299(1) Å]. This compound exhibits luminescent properties at the orange spectral range with an emission maximum at approximately 26316 cm^{-1}. AuS_2CNH_2 is an example of a compound with an extended crystal structure showing luminescence, while the above given examples from the literature,[52–58] investigated with respect to luminescence, are molecular Au^I compounds. It seems to be necessary to investigate

* Dr. C. L. Teske
E-Mail: cteske@ac.uni-kiel.de
[a] Institute of Inorganic Chemistry
Christian-Albrechts-Universität zu Kiel
Max-Eyth-Str. 2
24118 Kiel Germany
Supporting information for this article is available on the WWW under **http://dx.doi.org/10.1002/zaac.202000306** or from the author.

especially further Au^{I}-3D structures in order to come perhaps later to a general conclusion about the relationship between the dimensionality of a structure and luminescence. In this context, a re-examination of $Ba[Au_2SnS_4]$, applying modern measurement methods, appeared to be worthwhile. Herein, we report about the results of a revised single crystal structure analysis, powder X-ray diffraction investigations based on synchrotron radiation data and luminescence properties observed irradiating the sample with UV light.

Experimental Section

Synthesis: The synthesis procedure was reported in our earlier work.[21] $Ba[Au_2SnS_4]$ formed during a solid state reaction from the mixture of the binary starting sulfides (BaS, Au_2S and SnS_2) in the temperature range 400–540 °C in sealed silica glass ampoules with the starting materials placed in sintered corundum crucibles. A sulfur excess is necessary (approx. 1 mol/formula mass of the end product) and the ampoules were sealed under reduced argon pressure. The investigations described here were carried out with a still available sample from the earlier work.

X-ray Powder Diffraction: Synchrotron powder X-ray diffraction was carried out at PETRA III, beamline P0.21[60] (DESY, Hamburg) with a wavelength of λ = 0.20712 Å. The sample was loaded in a 0.3 mm glass capillary. The instrumental resolution was determined by refinement of LaB_6 (NIST SRM 660c) as standard using a Thompson-Cox-Hastings pseudo-Voigt profile. Rietveld refinements were carried out using Topas Academic version 6.0.[61]

Single-crystal X-ray Investigation: A STOE Imaging Plate Diffraction System (IPDS-1) with graphite monochromatized Mo-K_α radiation (λ = 0.7107 Å) was used to collect single-crystal X-ray diffraction data of a red, needle shaped crystal at ambient temperature. After the correction of the raw data for Lorentz and polarization effects, the space group ($C222_1$, vide infra) was determined with the help of X-RED,[62] and the absorption correction was applied using X-RED and X-Shape[63] The SHELXL-2014 program package[64] was used for the location of the heavy atom positions from *Patterson* synthesis, and to solve the crystal structure. The final refinement with anisotropic displacement parameters was performed against F^2. Technical details of the data acquisition and selected refinement results are summarized in Table 1. The final atomic coordinates as well as the equivalent isotropic displacement parameters are listed in Table S1 (Supporting Information). Table 2 shows the list of selected shortest interatomic distances and bond angles.

Crystallographic data (including structure factors) for the structure in this paper have been deposited with the Cambridge Crystallographic Data Centre, CCDC, 12 Union Road, Cambridge CB21EZ, UK. Copies of the data can be obtained free of charge on quoting the depository number CCDC-2031831 (Fax: +44-1223-336-033; E-Mail: deposit@ccdc.cam.ac.uk, http://www.ccdc.cam.ac.uk).

Luminescence Measurements: Luminescence measurements were carried out with a FL322 Fluorolog-3 fluorescence spectrometer (HORIBA Jobin Yvon GmbH), containing a 450 W xenon lamp, a R928P photomultiplier, iHR-320-FA triple grating imaging spectrograph, and a Syncerity CCD detector. The solid $Ba[Au_2SnS_4]$ sample was measured at room temperature in Suprasil® quartz ampoule. The color coordinates were calculated from the measured luminescence spectra, applying the Software Origin®.[65]

Table 1. Crystal data and structure refinement for $Ba[Au_2SnS_4]$.

	$Ba[Au_2SnS_4]$
Empirical formula	$Au_8\ Ba_4\ S_{16}\ Sn_4$
Formula weight	3112.88
Temperature /K	298(3)
Wavelength /Å	0.71073
Crystal system	orthorhombic
Space group	$C222_1$
a /Å	6.6387(3)
b /Å	11.0605(7)
c /Å	10.9676(6)
Volume /Å^3	805.32(8)
Z	1
ρ (calculated) /g·m^{-3}	6.418
μ /mm^{-1}	45.144
$F(000)$	1312
Crystal size /mm^3	0.143 × 0.112 × 0.081
Θ range for data collection /°	3.579 to 28.249°
Reflections collected	4106
Independent reflections	999
$R_{(int)}$	0.0511
Completeness to Θ = 25°/%	100.0
Absorption correction	numerical
Max. /min. transmission	0.0385 / 0.0095
Refinement method	Full-matrix least-squares on F^2
Data / restraints / parameters	999 / 0 / 40
Goodness-of-fit on F^2	1.091
R_1 [$F_o > 4\sigma(F_o)$]	0.0363
wR_2 [$F_o > 4\sigma(F_o)$]	0.0976
R_1 (all data)	0.0385
wR_2 (all data)	0.0991
Absolute structure parameter	0.01(3)
Extinction coefficient	0.0020(3)
$\Delta\rho$ /e·Å^{-3}	1.901 / –1.423

Table 2. Selected bond lengths /Å and angles/° for $Ba[Au_2SnS_4]$ (standard deviations in parenthesis).

Ba–S	3.238(5) 2×
Ba–S	3.285(5) 2×
Ba–S	3.378(5) 2×
Ba–S	3.424(5) 2×
Au–S	2.314(5)
Au–S	2.324(5)
Sn–S	2.416(5) 4×
Au–Au	2.9538(13)
S–Au–S	177.3(2)
S–Sn–S	108.7(2)
S–Sn–S	106.6(2) 2×
S–Sn–S	113.6(2) 2×
S–Sn–S	107.9(2)

Supporting Information (see footnote on the first page of this article): Atomic coordinates (Table S1). Comparison of the BS8 polyhedra for some selected thiostannates (Table S2))

Results and Discussion

$Ba[Au_2SnS_4]$ crystallizes in the orthorhombic space group $C222_1$ (no. 20), and the C-centering is unambiguously present which was overlooked in[21] where the space group $P2_12_12$ was reported. The inspection of the polycrystalline product indicated that a minor impurity phase is present. For semi-quantitative determination of the side-phase in-house X-ray

data collected with Cu-Kα radiation are not suitable due to the pronounced absorption of X-rays. Even in a thin capillary of 0.3 mm diameter, the absorption coefficient μ*r* is ca. 11, preventing a reliable determination of the amount of the side-phase. Hence, we decided measuring an X-ray powder pattern using hard X-rays available at P02.1 (DESY) allowing collecting data of high quality with negligible absorption effect (μ*r* ≈ 0.25), which are also suitable for a Rietveld refinement. The refinement (Figure 1) was only successful using the space group $C222_1$ supporting the results of single crystal structure determination. We note that the lattice parameters obtained by the Rietveld refinement agree well with that determined on a single crystal. Moreover, the Rietveld refinement resulted in a contamination of the product by about 13 % elemental Au and a small amount of an unidentifiable by-product.

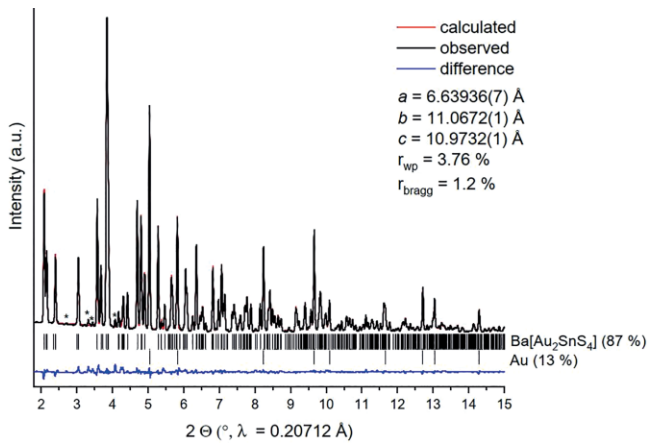

Figure 1. Result of the Rietveld refinement of X-ray data collected at DESY (λ = 0.20712 Å). Vertical bars indicate the positions of Bragg reflections. Impurity lines from an unknown compound are marked with an asterisk.

In the crystal structure the unique Sn^{4+} cation is surrounded tetrahedrally (Figure 2) by four S^{2-} anions with Sn–S bond length of 2.416(5) Å, which is comparable with bond lengths in other related thiostannates.[19–22] The sum of the ionic radii is Σ = r(Sn^{4+}) + r(S^{2-}) = 2.39 Å,[66] and the experimental bond length agrees well with this value. The S–Sn–S angles indicate a moderate distortion of the tetrahedron (Table 2). The unique Au^{+} cation is linearly coordinated in a dumbbell-like fashion (Figure 1) with Au–S bond lengths of 2.314(5) and 2.324(5) Å. The S–Au–S angle of 177.3(2)° indicates a small deviation from linearity. (see Table 2). Deviations from linearity of the S–Au–S angle have been mentioned earlier in the literature, e.g. for $Cs_2Au_2SnS_4$ 173.8°,[42] for $K_2Au_2SnS_4$ 175.1°, 174.6°, for $K_2Au_2Sn_2S_6$ 175,4°,[43] for $Au_2[S_2CN(C_2H_5)_2]_2$ 177.1°, 176.8°,[67] for $[Au(mpdtc)]_2$ 171.3° –172.5°[56] [(mpdtc) = methyl(2-(pyridin-2-yl)ethyl)dithiocarbamate], and for $Tl_2Au_2S_3$ 175°.[68]

The intra-chain Au···Au separation of 2.9538(13) Å is only slightly longer than in elemental Au (2.8782 Å),[44] whereas the inter-chain Au···Au separation is longer at 3.383 Å. The AuS_2 dumbbells connect two adjacent SnS_4 tetrahedra, as depicted in Figure 2. This connection scheme generates chains $[(Au_2SnS_4)^{2-}]_\infty$ propagating in the [100] direction (Figure 2).

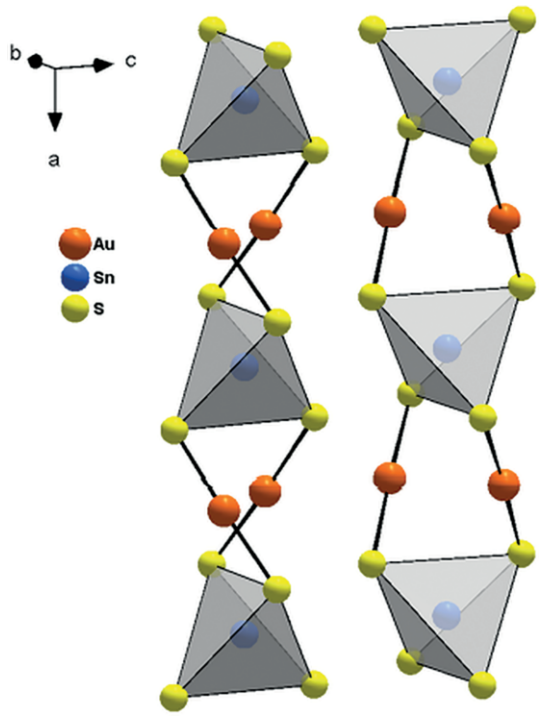

Figure 2. Interconnection of the SnS_4 tetrahedra and the AuS_2 dumbbells generating chains $[(Au_2SnS_4)^{2-}]_\infty$.

The Ba^{2+} cations are in a distorted archimedic anti-prismatic or bicapped trigonal prismatic environment. The mean Ba–S bond length of 3.331(5) Å (Table 2) corresponds to the sum of the ionic radii [Σ r(Ba^{2+}) + r(S^{2-}) = 3.26 Å[66]]. The BaS_8 polyhedra are joined by corner-sharing of all eight S^{2-} anions forming a three dimensional network (Figure 3, top). This network contains channels along [100] hosting the $[(Au_2SnS_4)^{2-}]_\infty$ chains (Figure 3, bottom).

Due to the strong distortion the description of the geometry of coordination polyhedron (BaS_8) is not straightforward. However, when compared with some selected thiostannates, compositional variants of the TlSe type,[69] which have a tetrahedral framework structure, a special feature can be identified. Table S2 (Supporting Information) shows the Ba–S distances for seven examples. In five of these all Ba-S distances are relatively close to the mean values in the range of 3.22 to 3.33 Å. In contrast for $Ba[Au_2SnS_4]$ two Ba–S bonds at 3.424(5) Å are clearly outside this range. For $Ba_3[CdSn_2S_8]$ [70(e)] this is even more pronounced with 3.510(6) Å. In these cases the description of the BaS_8 polyhedron as a bicapped trigonal prism is possibly more appropriate. The volume and shape parameter *S* of the Ba polyhedron was calculated using the minimum bounding ellipsoid (MBE) approach[71] yielding *V* = 151.2 $Å^3$ and *S* = –0.17, indicating that the polyhedron is axially compressed. For Sn the volume is 58.8 $Å^3$ and *S* = –0.05, indicating only a small axial compression of the tetrahedron. We analyzed the six compounds listed in Table S2 (Supporting Information) with the MBE method. While the volumes of the SnS_4 tetrahedra show no pronounced variation (54.7–56.8 $Å^3$) indicating a relatively rigid behavior, the volumes of the BaS_8 polyhedra are much more variable with vol-

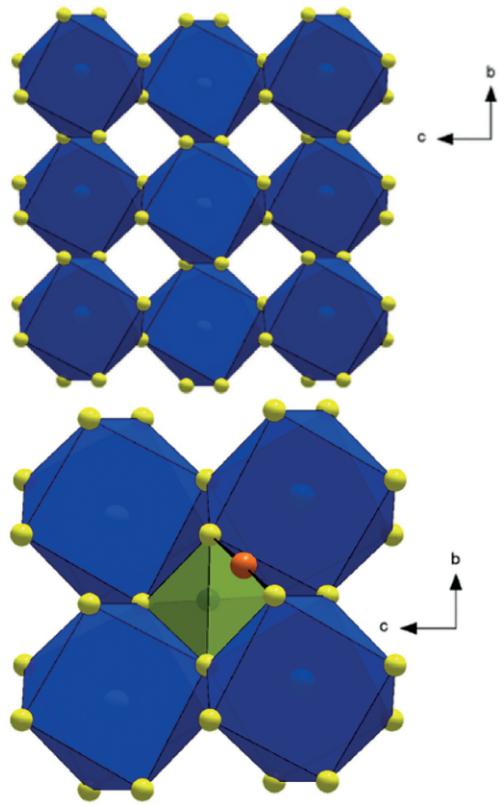

Figure 3. Polyhedral representation of the three-dimensional network generated by corner-sharing of the BaS_8 polyhedra (top) and location of the SnS_4 tetrahedra and Au^+ cations (bottom).

umes between 132.8 Å^3 and 150.4 Å^3, i.e. the Ba^{2+} environment is flexible adapting the structural packing requirements of the different constituents. The construction of the crystal structure is reminiscent of that of $KFeS_2$[72,73] and the structural principle reported for TlSe[69] or TlS, respectably.[74] In these compounds chains made of edge-sharing tetrahedra are observed. However, the AuS_2 dumbbells replace every second tetrahedron in the chains, respectively. The Au–Au distance obtained here is the shortest compared to the values reported for the other three thiostannates mentioned above, with Au–Au = 3.13091(13) Å for $Cs_2Au_2SnS_4$,[42] having an isostructural framework Au–Sn–S to the title compound, and $K_2Au_2SnS_4$ [Au–Au = 3.363(2) Å, 3.929(2) Å and 4.015(3) Å], and $K_2Au_2Sn_2S_6$ [Au–Au = 3.010(2) Å].[43] The latter two compounds have different structural frameworks compared to the title compound.

The emission spectrum of $Ba[Au_2SnS_4]$ (Figure 4, $\tilde{\nu}_{ex}$ = 34483 cm^{-1}) is composed mainly by a broad band distributed between approximately 17500 cm^{-1} and 27000 cm^{-1} with a maximum at 21000 cm^{-1}, whereas the excitation band is located at the energy range > 25000 cm^{-1} (Figure 4, $\tilde{\nu}_{em}$ = 22222 cm^{-1}). These optical properties result in the luminescence at the blue-green spectral range, with Commission internationale de l'éclairage (CIE) 1931[75] color coordinates of x = 0.1525 and y = 0.2834 (Figure 5). This luminescent behavior can be assigned to aurophilic interactions. Similar luminescence behavior for Au^I compounds was already reported in the literature, for instance, for the compounds $[Au(epdtc)]_2$,[56] $[Au(mpdtc)]_2$ [Au···Au: 2.7525(7)–2.7783(8) Å, $\lambda_{em,max}$ = 17778 cm^{-1}],[56] [C2mim][Au(SCN)$_2$],[76] $Au_2(NHC\text{-}(CH_2)_3\text{-}NHC)_2(PF_6)_2$[77] (Au···Au: 3.189 Å; $\lambda_{em,max}$ = 21187 cm^{-1}) $Au_2(NHC\text{-}(CH_2)_3\text{-}NHC)_2Br_2$[77] (Au···Au: 3.132 Å; $\lambda_{em,max}$ = 22728 cm^{-1}) [epdtc = ethyl(pyridine-4-ylmethyl)dithiocarbamate, mpdtc = methyl(2-(pyridin-2-yl)ethyl)dithiocarbamate, C_2mim = 1-alkyl-3-methylimidazolium]. As already mentioned in the introduction, it seems likely that with increasing Au–Au distances the emission energy declines and vice versa. However, this was shown e.g. for a series of bis(thiocyanato)-aurates(I)[58] and therefore, perhaps this is a special correlation not necessarily applicable to the title compound.

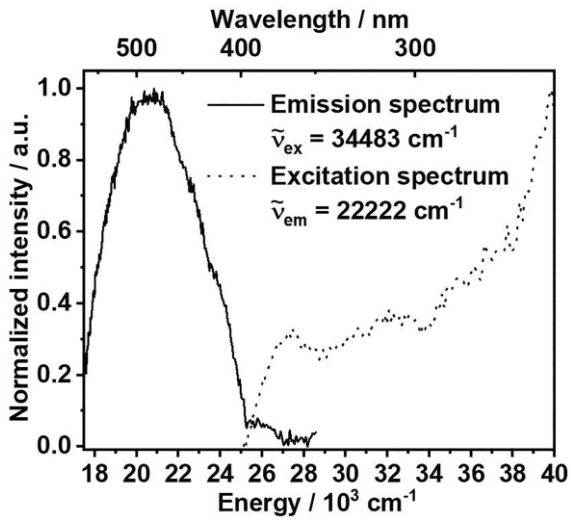

Figure 4. Emission ($\tilde{\nu}_{ex}$ = 34483 cm^{-1}, continuous curve) and excitation spectra ($\tilde{\nu}_{em}$ = 22222 cm^{-1}, dotted curve) of $Ba[Au_2SnS_4]$.

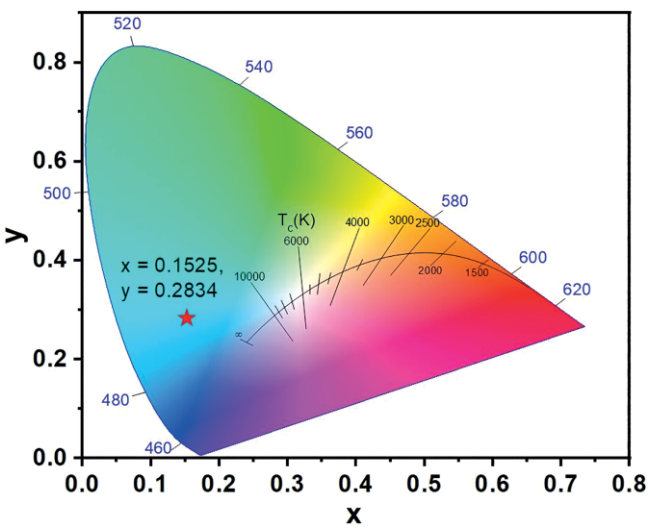

Figure 5. Plot of color coordinates of x = 0.1525, y = 0.2834 of $Ba[Au_2SnS_4]$ on the chromaticity diagram CIE 1931.[75]

Conclusions

We reinvestigated $Ba[Au_2SnS_4]$ motivated by our observation that even Au^I compounds with an extended structure show

luminescence properties. The results show that the true space group is $C222_1$ in contrast to what was reported earlier. While the main structural features are not significantly different to the model presented in,[21] several geometric parameters are significantly changed. In the structure the shortest Au···Au separation among the Au^I containing thiostannates is observed and the distance is only about 3 % longer than in elemental Au. An analysis of the related Ba^{2+} containing thiostannates demonstrates a rigid behavior of the SnS_4 tetrahedra while the BaS_8 polyhedron seems to be flexible reacting on the structural requirements of the other constituents by Ba–S bond lengths variation and distortion. In the former model the existence of a block structure was assumed, in which areas of the unit cells with identical arrangement superimpose with those twisted lengthwise [*001*] by 90° (note here we have different cell-orientation). This approach in fact led to significant distortions of the true coordination polyhedra though, not to fundamental changes in the structure principle of the crystal lattice. In any case, the present study with newly measured X-ray data has clearly shown that the description presented in reference[21] was inaccurate.

Actually, the compound tends to crystallize twinned. The structure could only be refined successfully as a 2-component inversion twin. Surely, this also applies to the data set of the old crystal used at that time (1978). $Ba[Au_2SnS_4]$ is a rare example of a three-dimensional material showing luminescence at the blue-green spectral range with emission maximum at approximately 21000 cm^{-1}. This seems plausible in comparison e.g. with the observed emission of AuS_2CNH_2, and the presumed correlation between the emission energy and the distance Au···Au (vide supra, introduction). Whether a relationship between the energy of the luminescence and the Au···Au separation can be established for three dimensional Au^I containing materials requires characterization of many more compounds. Finally, we would like to refer to two very recently published reviews,[78,79] which also seem interesting in connection with this article and the title compound. The first review deals with innovative molecular design strategies in materials science that follow the aurophillic concept. The latter refers to the fact that short Au···Au contacts are found that exhibit all kinds of multi-stimulus-induced light-emitting properties.

Acknowledgements

The authors are grateful to the institutions Deutsche Forschungsgemeinschaft (Project TE 1147/1–1), Bundesministerium für Bildung und Forschung and Bayerisches Staatministerium für Wissenschaft, Forschung und Kunst for covering the costs of the Electronic Journals Library and electronic databases (EZB). We acknowledge DESY (Hamburg, Germany), a member of the Helmholtz Association HGF, for the provision of experimental facilities. Parts of the research were carried out at PETRA III and we thank *Martin Etter* and *Alexander Schökel* for help in using beamline P02.1. Financial support by the State of Schleswig-Holstein is gratefully acknowledged. We thank *Inke Jeß* for the measurements of the single-crystal data. Open access funding enabled and organized by Projekt DEAL.

Keywords: X-ray diffraction; Gold; AuS_2 dumbbells; Aurophilicity; Luminescence properties

References

[1] Y. Ko, C. L. Cahill, J. B. Parise, *J. Chem. Soc., Chem. Commun.* **1994**, 69–70.
[2] G. A. Marking, M. Evain, V. Petricek, M. G. Kanatzidis, *J. Solid State Chem.* **1998**, *141*, 17–28.
[3] K. O. Klepp, F. Fabian, *Z. Naturforsch. B* **1999**, *54*, 1505–1509.
[4] B. Krebs, S. Pohl, W. Schiwy, *Angew. Chem.* **1970**, *82*, 884–885.
[5] W. S. Sheldrick, *Z. Anorg. Allg. Chem.* **1988**, *562*, 23–30.
[6] K. O. Klepp, *Monatsh. Chem.* **1984**, *115*, 1133–1142.
[7] B. Krebs, S. Pohl, W. Schiwy, *Z. Anorg. Allg. Chem.* **1972**, *393*, 241–252.
[8] D. Sarma, S. M. Islam, K. S. Subrahmanyama, M. G. Kanatzidis, *J. Mater. Chem. A* **2016**, *4*, 16597–16605.
[9] H. Lühmann, C. Näther, I. Jess, W. Bensch, *Z. Anorg. Allg. Chem.* **2019**, *645*, 1165–1170.
[10] G. A. Marking, J. A. Hanko, M. G. Kanatzidis, *Chem. Mater.* **1998**, *10*, 1191–1199.
[11] M. S. Devi, K. Vidyasagar, *J. Chem. Soc., Dalton Trans.* **2002**, 2092–2096.
[12] L. Garbato, A. Geddo-Lehmann, F. Ledda, *J. Cryst. Growth* **1991**, *114*, 299–306.
[13] O. Palchik, R. G. Iyer, C. G. Canlas, D. P. Weliky, M. G. Kanatzidis, *Z. Anorg. Allg. Chem.* **2004**, *630*, 2237–2247.
[14] Y. An, M. Ji, M. Baiyin, X. Liu, C. Jia, D. Wang, *Inorg. Chem.* **2003**, *42*, 4248–4249.
[15] M. Wu, T. J. Emge, X. Huang, J. Li, Y. Zhang, *J. Solid State Chem.* **2008**, *181*, 415–422.
[16] J. W. Lekse, B. M. Leverett, C. H. Lake, J. A. Aitken, *J. Solid State Chem.* **2008**, *181*, 3217–3222.
[17] A. S. Haynes, T.-K. Liu, L. Frazer, J.-F. Lin, S.-Y. Wang, J. B. Ketterson, M. G. Kanatzidis, K.-F. Hsu, *J. Solid State Chem.* **2017**, *248*, 119–125.
[18] J. Huang, X. Su, D. Hou, B. Lei, Z. Yang, S. Pan, *J. Solid State Chem.* **2017**, *249*, 215–220.
[19] C. L. Teske, *Z. Anorg. Allg. Chem.* **1976**, *419*, 67–76.
[20] a) C. L. Teske, *Z. Anorg. Allg. Chem.* **1976**, *427*, 200–204; b) C. L. Teske, O. Vetter, *Z. Anorg. Allg. Chem.* **1976**, *426*, 281–287.
[21] C. L. Teske, *Z. Anorg. Allg. Chem.* **1978**, *445*, 193–201.
[22] a) C. L. Teske, *Z. Anorg. Allg. Chem.* **1980**, *460*, 163–168; b) C. L. Teske, *Z. Naturforsch. B* **1980**, *35*, 7–11; c) C. L. Teske, *Z. Anorg. Allg. Chem.* **1985**, *522*, 122–130; d) C. L. Teske, *Z. Naturforsch. B* **1980**, *35*, 509–510.
[23] D.-X. Jia, Y. Zhang, J. Dai, Q.-Y. Zhu, Y.-M. Gu, *Z. Anorg. Allg. Chem.* **2004**, *630*, 313–318.
[24] X.-M. Gu, J. Dai, D.-X. Jia, Y. Zhang, Q.-Y. Zhu, *Cryst. Growth Des.* **2005**, *5*, 1845–1848.
[25] N. Pienack, W. Bensch, *Z. Anorg. Allg. Chem.* **2006**, *632*, 1733–1736.
[26] N. Pienack, C. Näther, W. Bensch, *Solid State Sci.* **2007**, *9*, 100–107.
[27] N. Pienack, K. Möller, C. Näther, W. Bensch, *Solid State Sci.* **2007**, *9*, 1110–1114.
[28] N. Pienack, A. Puls, C. Näther, W. Bensch, *Inorg. Chem.* **2008**, *47*, 9606–9611.
[29] N. Pienack, C. Näther, W. Bensch, *Eur. J. Inorg. Chem.* **2009**, 1575–1577.
[30] B. Zhang, M.-L. Feng, J. Li, Q.-Q. Hu, X.-H. Qi, X.-Y. Huang, *Cryst. Growth Des.* **2017**, *17*, 1235–1244.
[31] D. Friedrich, S. Greil, T. Block, L. Heletta, R. Pöttgen, A. Pfitzner, *Z. Anorg. Allg. Chem.* **2018**, *644*, 1707–1714.
[32] A. Benkada, H. Reinsch, W. Bensch, *Eur. J. Inorg. Chem.* **2019**, 4427–4432.

[33] J. Hilbert, C. Näther, W. Bensch, *Cryst. Growth Des.* **2017**, *17*, 4766–4775.
[34] J. Hilbert, C. Näther, W. Bensch, *Inorg. Chim. Acta* **2017**, *459*, 29–35.
[35] J. Li, B. Marler, H. Kessler, M. Soulard, S. Kallus, *Inorg. Chem.* **1997**, *36*, 4697–4701.
[36] P. Norby, E. Eikeland, J. Overgaard, S. Johnsen, B. B. Iversen, *CrystEngComm* **2015**, *17*, 2413–2420.
[37] S. Dehnen, C. Zimmermann, *Z. Anorg. Allg. Chem.* **2002**, *628*, 2436–2439.
[38] M. Ø. Filsø, I. Chaaban, A. Al Shehabi, J. Skibsted, N. Lock, *Acta Crystallogr., Sect. B* **2017**, *73*, 931–940.
[39] L. Nie, Y. Zhang, K. Ye, J. Han, Y. Wang, G. Rakesh, Y. Li, R. Xu, Q. Yan, Q. Zhang, *J. Mater. Chem. A* **2015**, *3*, 19410–19416.
[40] MS Hvid, H. S. Jeppesen, M. Miola, P. Lamagni, R. Su, K. M. Ø. Jensen, N. Lock, *IUCrJ* **2019**, *6*, 804–814.
[41] X.-H. Qi, K.-Z. Du, M.-L. Feng, Y.-J. Gao, X.-Y. Huang, M. G. Kanatzidis, *J. Am. Chem. Soc.* **2017**, *139*, 4314–4317.
[42] S. Löken, W. Tremel, *Z. Anorg. Allg. Chem.* **1998**, *624*, 1588–1594.
[43] J.-H. Liao, M. G. Kanatzidis, *Chem. Mater.* **1993**, *5*, 1561–1569.
[44] W. B. Pearson, *A Handbook of Lattice Spacings and Structures of Metals and Alloys*, Part II, Pergamon Press, London, **1964**, p. 124.
[45] Y. Jiang, S. Alvarez, R. Hoffmann, *Inorg. Chem.* **1985**, *24*, 749–757.
[46] M. Jansen, *Angew. Chem.* **1987**, *99*, 1136–1146.
[47] F. Scherbaum, A. Grohmann, B. Huber, C. Krüger, H. Schmidbaur, *Angew. Chem.* **1988**, *100*, 1602–1604.
[48] H. Schmidbaur, *Gold Bull.* **1990**, *23*, 11–33.
[49] H. Schmidbaur, *Gold Bull.* **2000**, *33*, 1–33.
[50] P. Pyykkö, *Angew. Chem. Int. Ed.* **2004**, *43*, 4412–4456; P. Pyykkö, *Inorg. Chim. Acta* **2005**, *358*, 4113–4130; P. Pyykkö, *Chem. Soc. Rev.* **2008**, *37*, 1967–1997.
[51] H. Schmidbaur, A. Schier, *Chem. Soc. Rev.* **2008**, *37*, 1931–1951; H. Schmidbaur, A. Schier, *Chem. Soc. Rev.* **2012**, *41*, 370–412.
[52] C. King, J.-C. Wang, M. Nazrul, I. Khan, J. P. Fackler Jr., *Inorg. Chem.* **1989**, *28*, 2145–2149.
[53] M. Bardaji, A. Laguna, P. G. Jones, A. K. Fischer, *Inorg. Chem.* **2000**, *39*, 3560–3566.
[54] E. E. Langdon-Jones, S. J. A. Pope, *Chem. Commun.* **2014**, *50*, 10343–10354 and references cited therein.
[55] X. He, V. W.-W. Yam, *Coord. Chem. Rev.* **2011**, *255*, 2111–2123.
[56] S. Han, O. S. Jung, Y. A. Lee, *Transition Met. Chem.* **2011**, *36*, 691–697.
[57] Z. Assefa, B. G. McBurnett, R. J. Staples, J. P. Fackler Jr., B. Assmann, K. Angermaier, H. Schmidbaur, *Inorg. Chem.* **1995**, *34*, 75–83.
[58] N. L. Coker, J. A. Krause Bauer, R. C. Elder, *J. Am. Chem. Soc.* **2004**, *126*, 12–13.
[59] C. L. Teske, H. Reinsch, H. Terraschke, W. Bensch, *Z. Anorg. Allg. Chem.* **2017**, *643*, 466–470.
[60] A.-C. Dippel, H.-P. Liermann, J. T. Delitz, P. Walter, H. Schulte-Schrepping, O. H. Seeck, H. Franz, *J. Synchrotron Radiat.* **2015**, *22*, 675–687.
[61] A. Coelho, *J. Appl. Crystallogr.* **2018**, *51*, 210–218.
[62] X-RED, Data Reduction Program, Version 1.11, Stoe & Cie GmbH, **1998**.
[63] X-SHAPE, Version 1.03, Stoe & Cie GmbH, Darmstadt, Germany, **1998**.
[64] SHELXL-2014-Crystal Structure Refinement-Multi-CPU Version 2014/7; G. M. Sheldrick, *Acta Crystallogr. Sect. A* **2008**, *64*, 112.
[65] Origin®, Version 2019b, www.OriginLab.com.
[66] R. D. Shannon, *Acta Crystallogr. Sect. A* **1976**, *32*, 751.
[67] D. D. Heinrich, J-C. Wang, J. P. Fackler Jr., *Acta Crystallogr., Sect. C* **1990**, *46*, 1444–1447.
[68] S. Löken, C. Felser, W. Tremel, *Chem. Commun.* **1998**, 1603–1604.
[69] J. A. A. Ketelaar, W. H. t' Hart, M. Moerel, D. Polder, *Z. Kristallogr.* **1939**, *101*, 396–405.
[70] a) C. L. Teske, *Z. Anorg. Allg. Chem.* **1976**, *427*, 200–204; b) C. L. Teske, *Z. Anorg. Allg. Chem.* **1980**, *460*, 163–168; c) C. L. Teske, *Z. Naturforsch. B* **1980**, *35*, 7–11; C. L. Teske, d) C. L. Teske, *Z. Naturforsch. B* **1980**, *35*, 509–510; e) C. L. Teske, *Z. Anorg. Allg. Chem.* **1985**, *522*, 122–130.
[71] J. Cumby, J. P. Attfield, *Nat. Commun.* **2016**, *8*, 14235.
[72] J. W. Boon, C. H. MacGillavry, *Recueil Trav. Chim. Pays-Bas* **1942**, *61*, 910–920.
[73] W. Bronger, *Z. Anorg. Allg. Chem.* **1968**, *359*, 225–233.
[74] H. Hahn, W. Klinger, *Z. Anorg. Allg. Chem.* **1949**, *260*, 110–119.
[75] K. M. M. K. Prasad, S. Raheem, P. Vijayalekshmi, C. Kamala Sastri, *Talanta* **1996**, *43*, 1187–1206.
[76] N. Aoyagi, Y. Shinha, A. Ikeda-Ohno, Y. Haga, K. Shimojo, N. R. Brooks, A. Izuoka, H. Naganawa, T. Kimura, K. Binnemans, *Cryst. Growth Des.* **2015**, *15*, 1422–1429.
[77] A. A. Penney, V. V. Sizov, E. V. Grachova, D. V. Krupenya, V. V. Gurzhiy, G. L. Starova, S. P. Tunik, *Inorg. Chem.* **2016**, *55*, 4720–4732.
[78] N. Mirzadeh, S. H. Priver, A. J. Blake, H. Schmidbaur, S. K. Bhargava, *Chem. Rev.* **2020**, *120*, 7551–7591.
[79] H. Schmidbaur, H. G. Raubenheimer, *Angew. Chem. Int. Ed.* **2020**, *59*, 14748–14771.

Received: August 18, 2020
Published Online: October 20, 2020